UC Berkeley
UC Berkeley Previously Published Works

Title
Reconciling Differences Between Large-Eddy Simulations and Doppler Lidar Observations of Continental Shallow Cumulus Cloud-Base Vertical Velocity

Permalink
https://escholarship.org/uc/item/67n607sd

Authors
Endo, Satoshi
Zhang, Damao
Vogelmann, Andrew M
et al.

Peer reviewed

Reconciling Differences Between Large-Eddy Simulations and Doppler Lidar Observations of Continental Shallow Cumulus Cloud-Base Vertical Velocity

Satoshi Endo1 , Damao Zhang1 , Andrew M. Vogelmann1 , Pavlos Kollias1,2 , Katia Lamer3 , Mariko Oue2 , Heng Xiao4 , William I. Gustafson Jr4 , and David M. Romps5,6

1 Environmental and Climate Sciences Department, Brookhaven National Laboratory, Upton, NY, USA, 2 School of Marine and Atmospheric Sciences, Stony Brook University, Stony Brook, NY, USA, 3 Earth and Atmospheric Sciences, The City College of New York, New York, NY, USA, 4 Atmospheric Sciences and Global Change Division, Pacific Northwest National Laboratory, Richland, WA, USA, 5 Department of Earth and Planetary Science, University of California, Berkeley, CA, USA, 6 Climate and Ecosystem Sciences Division, Lawrence Berkeley National Laboratory, Berkeley, CA, USA

Correspondence to: S. Endo, sendo@bnl.gov

Abstract

We investigate a significant model-observation difference found between cloud-base vertical velocity for continental shallow cumulus simulated using large-eddy simulations (LES) and observed by Doppler lidar measurements over the U.S. Southern Great Plains Atmospheric Radiation Measurement Facility. The LES cloud-base vertical velocity is dominated by updrafts that are consistent with a general picture for convective clouds but is inconsistent with Doppler lidar observations that also show the presence of considerable downdrafts. The underestimation of simulated downdrafts is found to be a robust feature, being insensitive to various numerical, physical, or dynamical choices. We find that simulations can more closely reproduce observations only after improving the model physics to use size-resolved microphysics and horizontal longwave radiation, both of which modify the cloud buoyancy and velocity structure near cloud side edges. The results suggest that treatments that capture these structures are needed for the proper simulation and subsequent parameterization development of shallow cumulus vertical transport.

Plain Language Summary

Cumulus clouds are important to vertical transport and the heat and moisture budgets in the lower atmosphere. The representations of these clouds in weather and climate models are typically based on studies using higher-resolution models. However, we use observations to show that high-resolution models normally do not properly simulate the vertical wind at cloud bottom that governs cloud evolution. We demonstrate that models can closely match the observed vertical winds at cloud bottom by improving the model physics to compute cloud droplet evolution explicitly for a range of droplet sizes while also computing the cooling at cloud sides caused by the

horizontal emission of infrared radiation. These improvements enhance downdrafts near cloud sides and bring the simulations in line with observed vertical velocity statistics at cloud bottom.

1 Introduction

Cloud-base vertical velocity is critical to the evolution of shallow cumulus clouds. It is an outcome of subcloud-layer dry convection, driven by the surface buoyancy flux, and cloud layer moist convection, driven by condensational heating. Vertical velocity at cloud base produces the fluxes of scalars and momentum at the interface between the subcloud boundary layer and the atmosphere at higher levels. Thus, it plays a major role controlling vertical transport in the lower atmosphere that must be properly represented in parametrizations developed for numerical weather prediction and climate models.

Despite the importance of cloud-base vertical velocity, earlier studies suggest an inconsistency between measured and simulated vertical velocities. Large-eddy simulations (LES) are often used to understand cloud and boundary layer processes. LES-produced cloud-base vertical velocity is generally dominated by updrafts (e.g., Chen et al., 2012; Couvreux et al., 2010; Sakradzija & Hohenegger, 2017), consistent with a general picture of convective clouds initiated by updrafts at cloud base. In contrast, observational studies based on long-term statistics report that at cloud base of continental shallow convection, the downdrafts can be as frequent as updrafts (Chandra et al., 2013; Lamer & Kollias, 2015; Lareau et al., 2018). This inconsistency suggests that LES may underestimate downdraft frequency at cloud base, which may affect our understanding and bias parameterizations of vertical transport in the lower atmosphere.

The U.S. Department of Energy's Atmospheric Radiation Measurement (ARM) user facility has started routine operation of LES for shallow cumulus convection over the Southern Great Plains (SGP) atmospheric observatory. The LES ARM Symbiotic Simulation and Observation Workflow (LASSO) project provides a growing library of continental shallow cumulus cases intended to bridge the gap between observations and models for the improvement of physical parameterizations in large-scale models, among other goals (Gustafson et al., 2017a). ARM supports LASSO with enhanced profiling observations including vertical velocity measurements by a Doppler lidar (DL) network at the SGP. The deployment of the operational LES and the DL network provides the means to explore the model-observation difference in the cloud-base vertical velocity of shallow cumulus clouds.

This study capitalizes on these new modeling and observational capabilities to investigate the difference between observed and simulated cloud-base vertical velocities of continental shallow cumulus clouds. Further, LES sensitivity studies are performed to reconcile simulated and observed cloud-base vertical velocities to identify model deficiencies responsible for the discrepancies from the observations.

2 Data Sets and Sampling Methodology

A network of five DLs is deployed at the ARM SGP site providing long-term, continuous observations of atmospheric boundary layer and cloud processes since May 2016. DL measurements provide profiles of vertical velocity and attenuated backscatter from atmospheric particles such as aerosols and cloud droplets. One instrument is at the Central Facility, and the other four are at extended facilities located within a 50-km radius around the Central Facility (see Supporting Information for a map). The configuration of the ARM lidars yields a vertical resolution of 30 m, a temporal resolution of approximately 1.5 s, and a vertical velocity uncertainty ~0.1 m/s (Newsom, 2012).

The DL measurements from the five sites are analyzed to obtain statistics of cloud-base vertical velocity for fair-weather shallow cumulus clouds both over the long term and for specific LASSO case days. The long-term statistics are examined using 2 years of data from the five sites during daytime (0800–1800 local time) for the May–September periods of 2016–2017. Ten LASSO case days in 2016 are used in the analysis (05/18, 06/10, 06/11, 06/19, 06/25, 07/19, 07/20, 08/18, 08/19, and 08/30). Identification of shallow cumulus clouds for the long-term statistics follows Lamer and Kollias (2015) which parallels Zhang and Klein (2013). In short, hours with shallow cumulus clouds are identified using four criteria: (1) presence of low-level clouds with cloud top below 4 km; (2) low-level cloud fraction between 3% and 60%; (3) absence of high-coverage low-level clouds with cloud chord length >5 km, where chord length is cloud duration multiplied by horizontal wind speed based on sounding; and (4) absence of rain measured by disdrometer and KAZR (reflectivity <0 dBZ) at the Central Facility. Since there is no radar at extended facilities, we use DL measurements to detect cloud boundaries.

In the hours selected for the long-term statistics and daytime of LASSO case days, cloud-base occurrences that are coupled to the subcloud layer are identified through a multi-step screening process designed to remove upper-level clouds and elevated cloud sides. First, a candidate cloud-base point is determined in each observed column from the DL attenuated backscatter profile as the lowest altitude that exceeds a threshold of 6×10^{-5} $m^{-1} \cdot sr^{-1}$ (Hogan et al., 2004). Second, outlier points more than ±30% away from the lifting condensation level (LCL) are removed from consideration. Third, for each DL site, the time series of the cloud-base height for each day is modeled as a quadratic function of time, with the three parameters of the quadratic chosen to give the best fit to the day's worth of cloud-base points from that DL site. Finally, cloud-base points that are within −200 and +100 m from the fit are considered to be connected to the subcloud layer and used for our analyses.

We performed several tests to examine potential uncertainties in the DL sampling methodology to find that results are invariant to multiple considerations (see Supporting Information for details). While a vertical

velocity PDF is sensitive to the definition of cloud base, the model-observation comparison depends only weakly on it.

We use simulations from the LASSO Alpha 2 release consisting of differently configured LES for shallow cumulus cases in 2016. In this release, LASSO provides LES ensembles including different large-scale forcings, horizontal resolutions, and LES models (see Gustafson et al., 2017b for further details). While we test various setting by using the LASSO library and additional simulations, a baseline configuration presented in this paper uses the Weather Research and Forecasting (WRF) model (Skamarock et al., 2008) with a horizontal grid spacing of 100 m, a vertical grid spacing of 30 m below 5 km, a horizontal domain size of 14.4 km, and a model top at 15 km. The physics suite uses Thompson microphysics (Thompson et al., 2008), Rapid Radiative Transfer Model for General Circulation Models (RRTMG) radiative transfer (Iacono et al., 2008), and 1.5-order Turbulence Kinetic Energy (TKE) subgrid-scale turbulence (Deardorff, 1980). The simulations are initialized with a sounding profile at 12 UTC (6 local time) and are driven for 15 hr by prescribed surface fluxes and large-scale forcings based on the ARM Variational Analysis (VARANAL) product (Xie et al., 2004). The simulated fields are saved every 10 min. Differences from this baseline configuration will be noted when applicable.

Simulated cloud-base vertical velocity is sampled similarly to the DL measurements except that the lowest cloudy point per model column is identified as the lowest model level with a threshold cloud water mixing ratio of 10^{-6} kg kg^{-6}. Like the lidar data analysis, the upper-level clouds and elevated cloud sides are removed by the same LCL-based criteria. Rather than defining a quadratic fit to the cloud base over each day, we simply use the mean of all the remaining cloud-base points at each instant in time. Vertical velocity is then sampled at cloud-base points that are located between −200 and +100 m from that average height. This procedure yields PDFs of vertical velocity that are nearly identical to the PDFs generated by using the same method that was applied to the observations (see Figure S2). The selected points occupy roughly the lowest 200 m of the 3-D cloud field, and the typical cloud thickness is around 3 km, so these vertical velocities may be considered "cloud-base vertical velocities."

3 Deficiency of LES Cloud-Base Vertical Velocity Identified Using Doppler Lidar Measurements

The PDFs of cloud-base vertical velocity are compared from the DL measurements and LASSO LES simulations for different periods (Figure 1a). General agreement between the "2-year" observed PDF (gray line) and the "10-day" observed PDF (black line) suggests that the 10 LASSO case days generally capture the long-term vertical velocity characteristics of the 2-year period. Compared to the 10-day observations, the 10-day LES PDF (red line) is shifted toward positive values. This shift indicates an underestimation in the frequency of downdrafts, with essentially no simulated downdrafts more

intense than -2 m/s^{-1}. This result confirms the model-observation difference anticipated from earlier modeling and observational studies.
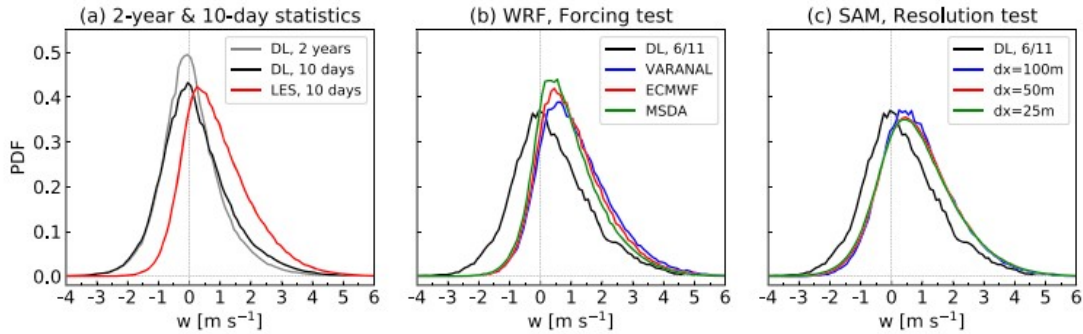
Figure 1. Probability density functions (PDFs) of cloud-base vertical velocity from Doppler lidar measurements and LASSO LES. (a) Measurements (black) and LES (red) for 10 LASSO case days in 2016 using WRF with the VARANAL large-scale forcing and 100-m horizontal grid spacing. Two-year statistics from the measurements are also shown (gray). (b) LASSO LES for 11 June 2016 using different large-scale forcings from VARANAL (blue), ECMWF (red), and MSDA (green) with same-day measurements (black). (c) LASSO LES for 11 June using SAM for different horizontal resolutions. SAM is forced by VARANAL with horizontal grid spacings of 100 (blue), 50 (red), and 25 m (green) alongside the same-day measurements (black).

Hereafter, we present results for the 11 June 2016 case, as the model-observation difference is consistent with the long-term statistics and a similar difference is apparent on any single day within the 10-day LASSO case set.

The sensitivity of simulated vertical velocity to the input large-scale forcing is explored using simulations from the LASSO LES library (Figure 1b). LASSO provides LES runs driven by several large-scale forcing data sets, generated for different forcing domain sizes from three independent data sources. We test simulations using forcings made with the largest region (300–413 km) from the three data sources: (1) VARANAL (our baseline) based on a variational analysis constrained by the Rapid Refresh analysis and the ARM observations (Xie et al., 2004); (2) the Integrated Forecast System operated by the European Centre for Medium-Range Weather Forecasts (ECMWF); and (3) regional WRF simulations constrained by a multiscale data assimilation (MSDA) technique (Li et al., 2015). The LES uses the large-scale forcing due to horizontal advection and vertical motion from each forcing data set; the surface fluxes are specified from the observation-based estimates included from the VARANAL product. As can be seen in Figure 1b, the PDFs of cloud-base vertical velocity are remarkably similar for the different large-scale forcings (colored lines), all of which maintain a consistent difference from the DL measurements (black line). The consistent difference is maintained despite changes in other simulated properties, such as cloud fraction and liquid water path (not shown).

The dependencies on the type of LES model and horizontal grid spacing are tested using simulations by the System for Atmospheric Modeling (SAM) model (Khairoutdinov & Randall, 2003), which are obtained from the LASSO

library. A key difference between the models is that SAM adapts an anelastic equation system for its dynamical core while WRF uses a fully compressible system. The SAM simulation uses the Morrison microphysics scheme (Morrison et al., 2009) and VARANAL large-scale forcing. Compared to the WRF simulation, the vertical velocity PDF for SAM is shifted slightly toward negative values, but the lack of downdrafts remains (compare the blue lines in Figures 1b and 1c). Smaller horizontal grid spacing is expected to improve the representation of entrainment mixing and downdrafts at the cloud sides. However, Figure 1c shows a negligible effect of decreasing horizontal grid spacing from 100 m (blue line) to 50 m (red line) and 25 m (green line). This result does not rule out the possibility that further resolution refinement might lead to improvement, but the apparent convergence of the results for 25 and 50 m of grid spacings is not encouraging.

Taken together, these tests confirm the LES-observation difference anticipated from previous research by using the LASSO LES library combined with DL measurements. We show that the lack of simulated cloud-base downdrafts is a remarkably robust feature, being insensitive to the day simulated, or the choice of large-scale forcing, LES model, or horizontal grid spacing.

4 Cause Attribution Using LES Sensitivity Tests

In this section, we test the sensitivity of LES cloud-base vertical velocity to changes in model physics that may improve the lack of simulated cloud-base downdrafts. While subcloud-layer dry convection is the significant contributor to the cloud-base updrafts in the PDF, the lack of downdrafts is likely related to cloud processes at higher altitudes. Earlier studies have investigated subsiding shells—which are a sheath of dry downdraft in the clear air next to the cloud side—using observations (Jonas, 1990; Rodts et al., 2003) and LES (Heus et al., 2009; Heus & Jonker, 2008; Jonker et al., 2008). These analyses indicate that cooling from droplet evaporation at upper levels is a main source of negative buoyancy driving the dry downdrafts (Heus & Jonker, 2008; Rodts et al., 2003). Although the subsiding shell is a downdraft outside the cloud, the insights from these studies help guide our investigation into physical processes that may play a role in representing downdrafts inside the cloud.

The literature suggests two promising candidates for enhancing downdrafts at cloud edge: the use of spectral-bin microphysics, and treating the horizontal longwave radiation. First, previous studies indicate the general importance of size-resolved microphysics to representing microphysical and macrophysical properties of shallow cumulus convection (e.g., vanZanten et al., 2011). More specifically, Zhang et al. (2017) report that the simulated ratio of in-cloud downdraft-to-updraft fraction in continental shallow cumulus is more realistic when using spectral-bin microphysics than when using a bulk microphysics scheme. Second, earlier work has shown that treating 3-D longwave radiation can lead to radiative cooling at cloud sides that causes

stronger downdrafts and increased entrainment (Guan et al., 1997; Klinger et al., 2017). We tested other model physics and numerical options in WRF through a suite of model sensitivity studies (see Supporting Information); however, the agreement of the simulated PDF of cloud-base vertical velocity with observations did not improve. Given the results, we focus on treating droplet-size-resolved microphysics and horizontal longwave radiation, which could play a role in any shallow cumulus simulation.

The sensitivity tests for droplet-size-resolved microphysics and horizontal longwave radiation are conducted with our baseline case using VARANAL forcing and 100-m horizontal grid spacing. The effect of size-resolved microphysics is tested using an updated version of the Hebrew University fast spectral-bin microphysics scheme (HUJI; Khain et al., 2010) that is available in WRF, in which the droplet size distribution is simulated using 33 mass bins (these simulations are referred to as SBM). The effect of horizontal longwave radiation is tested using a simple, computationally efficient scheme that includes the heating rate due to horizontal flux div/convergence to the existing heating rate from vertical fluxes from the RRTMG scheme similar to Guan et al. (1997; see Supporting Information for details); these simulations are referred to as HorLW.

The sensitivity of cloud-base vertical velocity to spectral-bin microphysics and horizontal longwave radiation is shown in Figure 2. We find that the spectral-bin microphysics and horizontal longwave radiation separately increase the frequency of downdrafts at the cloud base for the 11 June case (Figure 2a). Compared to our baseline (blue line), the shift due to size-resolved microphysics (orange line) is larger than that from horizontal longwave radiation (green line). When the size-resolved microphysics and horizontal longwave radiation are used in the same simulation (red line), the downdraft frequency significantly increases to more closely match the observations (black line), although there is still a tendency to slightly underestimate the downdrafts. Similar sensitivities can also be seen for another LASSO case day on 18 August (Figure 2b) and for widely used reference cases developed by (GEWEX) Cloud System Study (GCSS) (see Supporting Information). These results suggest that the combined effects of these two processes—both of which are typically not treated in LES for shallow convection—are important to accurately produce cloud-base vertical velocity.
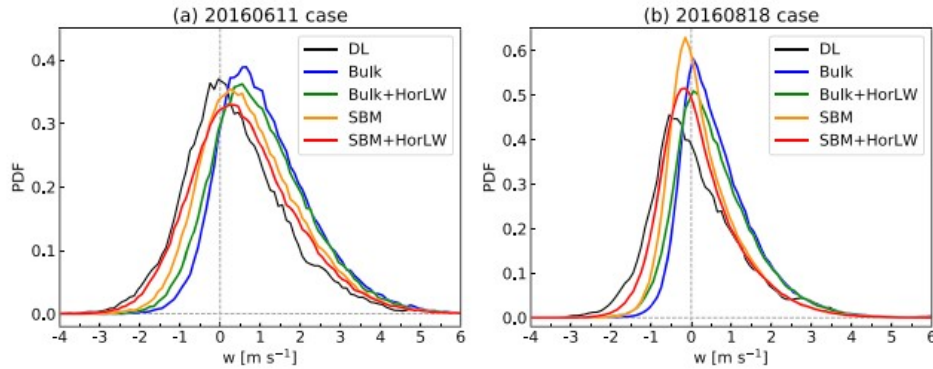
Figure 2. Probability density functions (PDFs) of cloud-base vertical velocity from LES testing combinations of bulk microphysics (Bulk), spectral-bin microphysics (SBM), and horizontal longwave radiation (HorLW). Simulations are for (a) 11 June 2016 and for (b) 18 August 2016.

The 11 June simulations are further analyzed to determine how the spectral-bin microphysics and horizontal longwave radiation may affect the physical state near cloud sides and how this may lead to the improved cloud-base vertical velocity statistics. The cloud-edge statistics are calculated for the period from 1300 to 1600 local time for two height ranges: one representing "cloud-base" height, within ±50 m from the LCL, and one for "midlevel," within ±50 of 600 m above the cloud-base height (i.e., LCL + 550 m < z < LCL + 650 m). Cloud sides are identified by scanning the layers in four directions: from west to east, from south to north, and in reverse for each. Variables are sampled along the scan direction in continuous eight-grid-point segments, consisting of four clear-air and four cloudy grid points where cloud edge is the outermost cloudy grid point.

The cloud-edge statistics of cloud water, relative humidity, buoyancy perturbation, and vertical velocity for the midlevel and cloud-base level are shown in Figure 3. A basic structure of shallow cumulus clouds can be seen for all simulations where cloud water, in-cloud buoyancy, and vertical velocity increase with height. Cloud water mixing ratio increases with height and inwards from the cloud edge (Figure 3a). Relative humidity is high in clouds (Figure 3b), and the maximum relative humidity in SBM reaches supersaturation. Buoyancy perturbations are slightly negative at cloud base (Figure 3c) because subcloud layer updrafts overshoot their level of neutral buoyancy, rising into the cloud layer that has large buoyancy. Consistent with the PDFs in Figure 2, cloud-base downdrafts at the outermost cloudy points (Figure 3d) are intensified most in the SBM+HorLW simulation, followed by SBM, Bulk+HorLW, and Bulk. These statistics are near the cloud sides and not exactly at cloud base, as in Figure 2; however, vertical velocity at cloud edges has a significant impact on area-weighted statistics such as PDFs because of the large area of the outer cloud area.
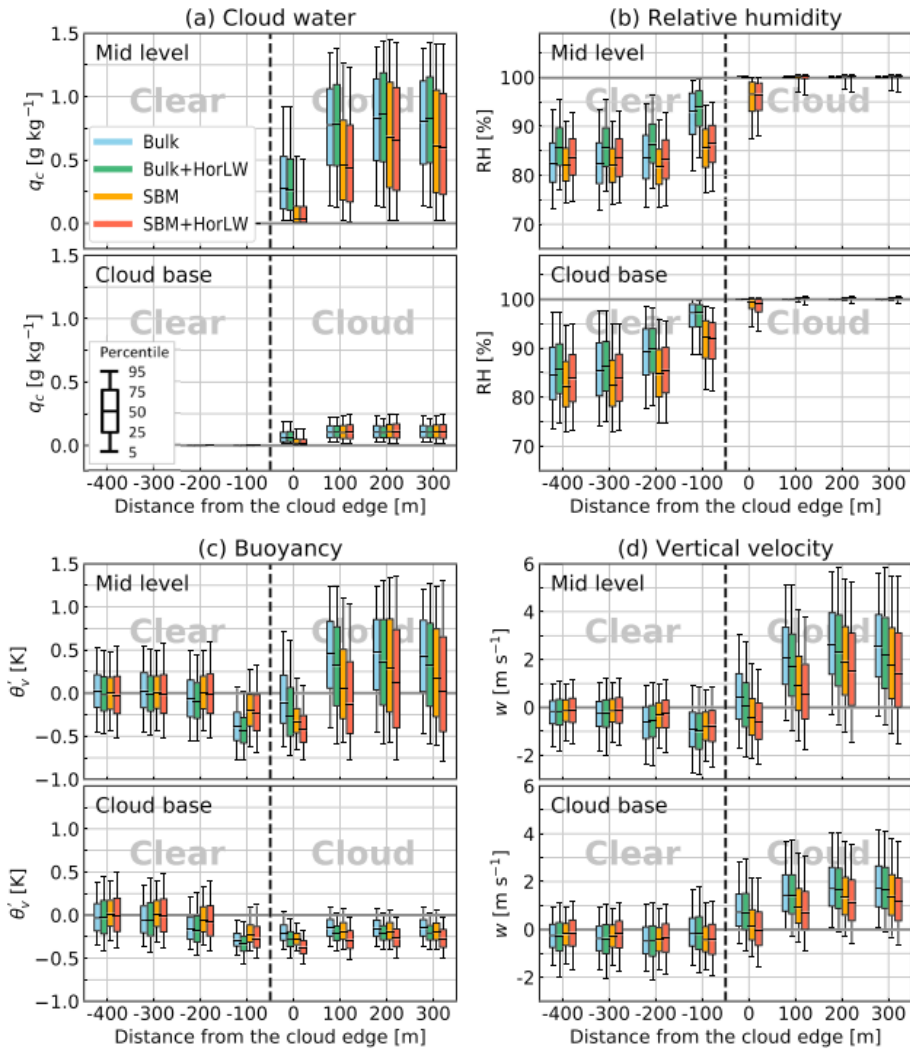
Figure 3. Cloud-edge statistics for the 11 June simulations shown in Figure 2 for (a) cloud water mixing ratio, (b) relative humidity, (c) buoyancy perturbation, and (d) vertical velocity. Shown are simulations using bulk microphysics (light blue), bulk microphysics with horizontal longwave radiation (green), spectral-bin microphysics (orange), and spectral-bin microphysics with horizontal longwave radiation (red). Statistics are provided for "cloud-base" height and "midlevel" (600 m above cloud base). The box and whiskers indicate, from the bottom, percentiles of 5, 25, 50, 75, and 95. The horizontal axis indicates the distance from the outermost cloudy grid point referred to as "cloud edge."

We first contrast the Bulk (blue, green) and SBM (orange, red) simulations. Looking at the top subpanels of Figure 3, the cloud-edge structure at midlevel is significantly different between the SBM and Bulk simulations. The Bulk simulations have completely saturated conditions everywhere in cloud (Figure 3b) and a greater decrease in mixing ratio values across the cloud boundary (Figure 3a) while, in contrast, the SBM simulations exhibit subsaturation accompanied by smaller liquid water mixing ratios at cloudy grid points near cloud edge. These differences in cloud-edge structure can be explained by how SBM and Bulk schemes treat droplet evaporation. The SBM scheme treats droplet evaporation in each bin such that droplets can exist during their evaporation in subsaturated air. The Bulk scheme, however,

employs a moist saturation adjustment scheme that instantaneously converts cloud water in subsaturated air into water vapor (if evaporation does not saturate the air). Based on a droplet growth model (Rogers & Yau, 1989), the evaporation of a 10-µm droplet in air with a temperature of 295 K and a fixed relative humidity takes 3.2 s at 85%, 4.9 s at 95%, and 49.8 s at 99%, which all exceed the 0.5-s LES timestep. Thus, the SBM scheme can have droplets present while evaporating in subsaturated air, whereas the Bulk scheme requires saturated air to maintain the droplets.

The ability of the SBM scheme (and inability of the Bulk scheme) to maintain a "cloudy" grid cell during droplet evaporation affects vertical velocity PDF because (1) droplet evaporation produces negative buoyancy which in turns produces downdrafts and (2) the subsaturated downdrafts can be classified as clouds because of the evaporating droplets they contain. Consistent with evaporative cooling expected from the cloud water and relative humidity distributions, the SBM midlevel buoyancy has a negative minimum at cloud edge, whereas the negative buoyancy minimum in the Bulk simulations occurs at the first clear-air grid point outside cloud edge (Figure 3c). The SBM simulations have the largest cloudy downdrafts at the cloud-edge grid point where the negative buoyancy is minimum, which should also be the case at other levels in the cloud layer. This dynamical effect together with the effect on "cloud classification" (by droplets existing in subsaturated air) explains why the SBM simulations have more cloudy downdrafts than Bulk at cloud base. We note that the effect of "cloud classification," although present, cannot explain the changes hundreds of meters into the cloud that must be due to the dynamical effect. It is interesting to note that the Bulk simulations that generate the negative buoyancy minimum outside the cloud produce more dry downdrafts at midlevels that, however, are significantly weakened at cloud-base height.

In contrast to the improvement by switching from bulk to size-resolved microphysics, the change experienced by using horizontal longwave radiation is more moderate, although still important. Horizontal longwave flux divergence is largest at cloud edge, where clouds lose radiation to be absorbed by the surrounding clear air (not shown). Simulations indicate that treating HorLW (green and red) or not (blue and orange) does not impact the cloud water distributions (Figure 3a), but treating it leads to the generation of more negative buoyancy and downdrafts within the clouds (Figures 3c and 3d, respectively). This makes sense since the diabatic cooling from the HorLW scheme enhances the negative buoyancy at cloud edges.

It is worthwhile discussing the potential importance of radiative cooling due to HorLW to help overcome a thermodynamic constraint to cloud-base downdraft occurrence due to parcel liquid water potential temperature (θ_l) conservation, where θ_l is equivalent to potential temperature when all the parcel cloud water evaporates and is conserved for adiabatic processes. An adiabatic parcel that rises from the cloud-base height due to condensational heating and then returns back down to that level due to evaporative cooling

has constant θ_l; thus, the parcel that returns to the cloud-base height does not have "extra cloud water" to produce more negative buoyancy and downdrafts at the cloud-base height. Mixing with environmental air further enhances the thermodynamic constraint. While mixing introduces dry air favorable to evaporative cooling, at the same time, it increases the parcel θ_l; this is equivalent to reducing the amount of negative buoyancy the parcel can potentially obtain when all the parcel cloud water evaporates, which prevents the parcel from reaching cloud-base height. The radiative cooling that reduces θ_l can help the parcel overcome the thermodynamic constraint and maintain negative buoyancy and downdrafts at cloud-base height.

5 Summary

Observations from the ARM SGP DL network and LASSO LES of continental shallow cumulus clouds are used to reconcile a significant difference found in simulated cloud-base vertical velocity when compared to observations. Analysis of the cloud-base vertical velocity PDF indicates that simulations lack enough downdrafts, which is a robust feature regardless of the choice of day or various model configurations such as the model resolution (down to 25 m) or large-scale forcing. Through the analysis of LES output at different distances from cloud edge and at different levels, we determined that the issue stems from a lack of simulated downdrafts at the cloud sides. The deficiency in LES downdrafts can be dramatically improved by introducing size-resolved microphysics combined with the horizontal longwave radiation. Treating these physical processes enhances evaporative cooling and radiative cooling at the cloudy points near the edge that intensifies the negative buoyancy and, as such, the occurrence of downdrafts that can reach the cloud-base height. The inclusion of these processes significantly improves the overall agreement of the simulated vertical velocity PDF with observations. A residual slight underestimation in downdraft frequency (and associated slight overestimation of the updraft frequency) suggests that unresolved influences may still remain from factors such as sampling or from untreated or mistreated model physics.

The focus of this paper is to diagnose the deficiency in simulated continental cloud-base downdrafts and propose a potential solution. The impacts of these physical processes on the cloud structure and life cycle would need further investigation; however, the results suggest that considering such physical processes that capture cloud buoyancy and velocity structure near cloud side edges are essential for net transport of mass, energy, and atmospheric constituents at cloud-base height and potentially at other levels. A bulk microphysics scheme not using saturation adjustment could better capture the aspects of the droplet evaporation represented by the spectral-bin microphysics. We note that the vertical velocity of marine cumuli is typically dominated by updrafts (Jonas, 1990; Kollias & Albrecht, 2010; Lamer et al., 2015; Rodts et al., 2003), differently from that for continental cumuli, so further investigation will be needed to understand the physics behind the marine-continental contrast and determine the potential effect of

our physical improvements. This research shows the continued need to use observations to assess the fidelity of LES that are often used as a reference for the parameterization development within the community. The results also emphasize the need for a dense observation network for generating reliable model diagnostics.

References

Chandra, A. S., Kollias, P., & Albrecht, B. A. (2013). Multiyear summertime observations of daytime fair-weather cumuli at the ARM Southern Great Plains Facility. *Journal of Climate*, 26(10), 031– 10,050. https://doi.org/10.1175/JCLI-D-12-00223.1

Chen, G., Xue, H., Feingold, G., & Zhou, X. (2012). Vertical transport of pollutants by shallow cumuli from large eddy simulations. *Atmospheric Chemistry and Physics*, 12, 11319– 11327. https://doi.org/10.5194/acp-12-11319-2012

Couvreux, F., Hourdin, F., & Rio, C. (2010). Resolved versus parametrized boundary-layer plumes. Part I: A parametrization-oriented conditional sampling in large-eddy simulations. *Boundary-Layer Meteorology*, 134, 441– 458. https://doi.org/10.1007/s10546-009-9456-5

Deardorff, J. W. (1980). Stratocumulus-capped mixed layers derived from a 3-dimensional model. *Boundary-Layer Meteorology*, 18, 495– 527. https://doi.org/10.1007/Bf00119502

Guan, H., Yau, M. K., & Davies, R. (1997). The effects of longwave radiation in a small cumulus cloud. *Journal of the Atmospheric Sciences*, 54, 2201– 2214. https://doi.org/10.1175/1520-0469(1997)054<2201:TEOLRI>2.0.CO;2

Gustafson, W. I., Vogelmann, A. M., Cheng, X., Endo, S., Krishna, B., Li, Z., Toto, T., & Xiao, H. (2017a). Recommendations for the implementation of the LASSO workflow. Technical Report, DOE/SC-ARM-17-031, DOE ARM Research Facility, 62 pp. https://doi.org/10.2172/1406259

Gustafson, W. I., Vogelmann, A. M., Cheng, X., Endo, S., Krishna, B., Li, Z., Toto, T., & Xiao, H (2017b). Description of the LASSO Alpha 2 Release.

Technical Report, DOE/SC-ARM-TR-199, DOE ARM Research Facility, 199 pp. https://doi.org/0.2172/1376727

Heus, T., & Jonker, H. J. J. (2008). Subsiding shells around shallow cumulus clouds. *Journal of the Atmospheric Sciences*, 65, 1003– 1018. https://doi.org/10.1175/2007JAS2322.1

Heus, T., Pols, C., Freek, J., Jonker, H. J. J., Van den Akker, H. E. A., & Lenschow, D. H. (2009). Observational validation of the compensating mass flux through the shell around cumulus clouds. *Quarterly Journal of the Royal Meteorological Society*, 135(638), 101– 112. https://doi.org/10.1002/qj.358

Hogan, R. J., Behera, M. D., O'Connor, E. J., & Illingworth, A. J. (2004). Estimate of the global distribution of stratiform supercooled liquid water clouds using the LITE lidar. *Geophysical Research Letters*, 31, L05106. https://doi.org/10.1029/2003GL018977

Iacono, M. J., Delamere, J. S., Mlawer, E. J., Shephard, M. W., Clough, S. A., & Collins, W. D. (2008). Radiative forcing by long-lived greenhouse gases: Calculations with the AER radiative transfer models. *Journal of Geophysical Research*, 113, D13103. https://doi.org/10.1029/2008JD009944

Jonas, P. R. (1990). Observations of cumulus cloud entrainment. *Atmospheric Research*, 25, 105– 127. https://doi.org/10.1016/0169-8095(90)90008-Z

Jonker, H. J. J., Heus, T., & Sullivan, P. P. (2008). A refined view of vertical transport by cumulus convection. *Geophysical Research Letters*, 35, L07810. https://doi.org/10.1029/2007GL032606

Khain, A., Lynn, B., & Dudhia, J. (2010). Aerosol effects on Intensity of landfalling hurricanes as seen from simulations with the WRF model with spectral bin microphysics. *Journal of the Atmospheric Sciences*, 67, 365– 384. https://doi.org/10.1175/2009JAS3210.1

Khairoutdinov, M. F., & Randall, D. A. (2003). Cloud resolving modeling of the ARM summer 1997 IOP: Model formulation, results, uncertainties, and sensitivities. *Journal of the Atmospheric Sciences*, 60, 607– 625. https://doi.org/10.1175/1520-0469(2003)060<0607:Crmota>2.0.Co;2

Klinger, C., Mayer, B., Jakub, F., Zinner, T., Park, S.-B., & Gentine, P. (2017). Effects of 3-D thermal radiation on the development of a shallow cumulus cloud field. *Atmospheric Chemistry and Physics*, 17, 5477– 5500. https://doi.org/10.5194/acp-17-5477-2017

Kollias, P., & Albrecht, B. (2010). Vertical velocity statistics in fair-weather cumuli at the ARM TWP Nauru Climate Research Facility. *Journal of Climate*, 23, 6590– 6604. https://doi.org/10.1175/2010JCLI3449.1

Lamer, K., & Kollias, P. (2015). Observations of fair-weather cumuli over land: Dynamical factors controlling cloud size and cover. *Geophysical Research Letters*, 42, 8693– 8701. https://doi.org/10.1002/2015GL064534

Lamer, K., Kollias, P., & Nuijens, L. (2015). Observations of the variability of shallow trade wind cumulus cloudiness and mass flux. *Journal of Geophysical Research: Atmospheres*, 120, 6161– 6178. https://doi.org/10.1002/2014JD022950

Lareau, N. P., Zhang, Y., & Klein, S. A. (2018). Observed boundary layer controls on shallow cumulus at the ARM Southern Great Plains site. *Journal of the Atmospheric Sciences*, 75, 2235– 2255. https://doi.org/10.1175/JAS-D-17-0244.1

Li, Z., Feng, S., Liu, Y., Lin, W., Zhang, M., Toto, T., Vogelmann, A. M., & Endo, S. (2015). Development of fine-resolution analyses and expanded large-scale forcing properties: 1. Methodology and evaluation. *Journal of Geophysical Research: Atmospheres*, 120, 654– 666. https://doi.org/10.1002/2014jd022245

Morrison, H., Thompson, G., & Tatarskii, V. (2009). Impact of cloud microphysics on the development of trailing stratiform precipitation in a simulated squall line: Comparison of one- and two-moment schemes. *Monthly Weather Review*, 137, 991– 1007. https://doi.org/10.1175/2008mwr2556.1

Newsom, R. K. (2012). Doppler lidar handbook. Technical Report, DOE/SC-ARM-TR-101, DOE ARM Research Facility, 16 pp. https://doi.org/10.2172/1034640

Rodts, S. M. A., Duynkerke, P. G., & Jonker, H. J. J. (2003). Size distributions and dynamical properties of shallow cumulus clouds from aircraft observations and satellite data. *Journal of the Atmospheric Sciences*, 60, 1895– 1912. https://doi.org/10.1175/1520-0469(2003)060<1895:SDADPO>2.0.CO;2

Rogers, R.R., & Yau, M.K. 1989: A short course in cloud physics. Butterworth-Heinemann, third edition, 304p.

Sakradzija, M., & Hohenegger, C. (2017). What determines the distribution of shallow convective mass flux through a cloud base? *Journal of the Atmospheric Sciences*, 74, 2615– 2632. https://doi.org/10.1175/JAS-D-16-0326.1

Skamarock, W. C., Klemp, J. B., Dudhia, J., Gill, D. O., Barker, D. M., Duda, M. G., Wang, W., & Powers, J. G. (2008). A description of the advanced research WRF version 3. NCAR Technical Note, NCAR/TN-475+STR, National Center for Atmospheric Research, 113 pp, https://doi.org/10.5065/D68S4MVH

Thompson, G., Field, P. R., Rasmussen, R. M., & Hall, W. D. (2008). Explicit forecasts of winter precipitation using an improved bulk microphysics scheme. Part II: Implementation of a new snow parameterization. *Monthly Weather Review*, 136, 5095– 5115. https://doi.org/10.1175/2008MWR2387.1

vanZanten, M. C., & Coauthors (2011). Controls on precipitation and cloudiness in simulations of trade-wind cumulus as observed during RICO.

Journal of Advances in Modeling Earth Systems, 3, M06001. https://doi.org/10.1029/2011MS000056

Xie, S. C., Cederwall, R. T., & Zhang, M. H. (2004). Developing long-term single-column model/cloud system-resolving model forcing data using numerical weather prediction products constrained by surface and top of the atmosphere observations. *Journal of Geophysical Research*, 109, D01104. https://doi.org/10.1029/2003jd004045

Zhang, Y., & Klein, S. A. (2013). Factors controlling the vertical extent of fair-weather shallow cumulus clouds over land: Investigation of diurnal-cycle observations collected at the ARM Southern Great Plains site. *Journal of the Atmospheric Sciences*, 70(4), 1297– 1315. https://doi.org/10.1175/JAS-D-12-0131.1

Zhang, Y., Klein, S. A., Fan, J., Chundra, A. S., Kollias, P., Xie, S., & Tang, S. (2017). Large-eddy simulation of shallow cumulus clouds over land: A composite case based on ARM long-term observations at its Southern Great Plains site. *Journal of the Atmospheric Sciences*, 74, 3229– 3251. https://doi.org/10.1175/JAS-D-16-0317.1